COMPRESSIVE STRENGTH OF COLUMNS WITH INITIAL DEFLECTIONS

Yuzuru Fujita
Professor
Department of Naval Architecture
University of Tokyo

Koichiro Yoshida
Associate Professor
Department of Naval Architecture
University of Tokyo

ABSTRACT

In this paper, the effects of initial deflections of columns on the compressive maximum loads are investigated, where columns are assumed to be under the combined states of axial compression and uni-axial bending.

The compression tests of 20 columns of rectangular section and 8 columns of H-type section with sine half wave type initial deflections were conducted.

The theoretical solutions were computed by using incremental Finite Element Method. The accordance of both results was satisfactory. Moreover, the maximum compressive loads of columns with irregular type of initial deflections and of eccentrically compressed columns with initial deflections were calculated theoretically.

1. INTRODUCTION

Structural elements of actual structures usually have several kinds of imperfections ; initial deflections, residual stresses, unexpected discontinuities of structural components and so on.

These imperfections may severely weaken the strength of structures designed based on the ideal states of structures. It is necessary to clarify the effects of imperfections not only qualitatively but also quantitatively. The theoretical analysis of the structures with imperfections, however, will not be easy in many cases partly because linear problems will become non-linear ones and in some cases two dimensional problems will become three dimensional ones and partly because it will be difficult to consider a suitable analytical models for so small amount of imperfections.

In this paper, the effects of initial deflections of columns on the compressive maximum loads are investigated theoretically and experimentally, where columns are assumed to behave under the combined states of axial compression and uni-axial bending. This is one of the most basic problems and studied by K. Jezek (1). However, as the comprehensive study on the effects of shapes and magnitudes of initial deflections on the compressive strength of columns seemed to be not enough, in this paper, authors applied the Finite Element Method to calculate the compressive maximum loads of columns with arbitrary shape of initial deflection and compared the results with the experiments in several cases.

2. COMPRESSION TESTS AND THEORETICAL CALCULATIONS OF COMPRESSIVE STRENGTH OF COLUMNS WITH INITIAL DEFLECTIONS

2.1. Compression Tests of Columns of Rectangular Section and H-type Section

The sectional dimensions of columns of rectangular section (hereafter, abbreviated to R-section) and of columns of H-type section (hereafter, abbreviated to H-section) were kept constant throughout specimens (see fig. 1) and the slenderness ratios were varied as follows ; 40, 60, 80, 100 and 120 for columns of R-section and 60 and 80 for columns of H-section. Initial deflections of specimens were formed by four points bending into the shape closely similar to half wave mode of sine curve and then stress relief was performed. (Hereafter, this type of initial deflections is called as a regular one). Four kinds of magnitudes of initial deflections were given for each slenderness ratio. Therefore, the total number of specimens was 28 pieces.

In the Fig. 2, the examples of measured initial deflections are shown. In the compression tests, the specimens were compressed by screw-type universal testing machine so that they might be bent about their weak axes with no rotational restraint at both ends.

These end conditions were attained by using end fixtures shown in the fig. 1.

2.2. Theoretical Calculation

Theoretical calculation was performed by the Finite Element Method because it is easy to deal with arbitrary shapes of initial deflections and with different kinds of end conditions. A column is divided into a number of beam elements and stiffness matrix of an element is calculated by assuming beam theory. To calculate the maximum load of a compressed column, it is necessary to trace its behaviour up to the stage of unloading after the maximum load attained. Therefore, the magnitude of both lateral deflection and axial strain of the column may become

considerably large.

In other words, both geometrical and material nonlinearity have to be simultaneously included in the theory. These two kinds of nonlinearity can be overcome approximately by the incremental load method which assumes piecewise linearity.

The errors due to this assumption are compensated approximately in this paper by modifying each load increment by the unbalance force at the previous step of configuration.

In the following, basic formulations for numerical calculations are given by using the general three dimensional finite displacement theory (2). When a body is deformed from some step of configuration to the adjacent step of configuration, the following relation may be assured from the principle of virtual work.

$$\frac{1}{2}\iiint_V \delta(\Delta\sigma_{\lambda\mu}\Delta\varepsilon_{\lambda\mu})dV + \frac{1}{2}\iiint_V \sigma_{\lambda\mu}\delta(\Delta u_{k,\lambda}\Delta u_{k,\mu})dV - \iiint_V \Delta\bar{X}_\lambda \delta\Delta u_\lambda dV$$

$$- \iint_{S_1} \Delta\bar{P}_\lambda \delta\Delta u_\lambda dS + \left(\iiint_V \sigma_{\lambda\mu}\delta\Delta\varepsilon_{\lambda\mu}dV - \iiint_V \bar{X}_\lambda \delta\Delta u_\lambda dV - \iint_{S_1} \bar{P}_\lambda \delta\Delta u_\lambda dS\right) = 0 \quad (1) \tag{1}$$

where Δ is a symbol to express an increment and $\bar{X}$ and $\bar{P}$ are body force and external force applied on force boundary S_1, respectively. $\Delta\varepsilon_{\lambda\mu}$ is a linear term of a strain increment expressed by finite displacement increments.

Assumption that external force, internal force and their increments are not varied during the variation with respect to displacement increment $\delta\Delta u_\lambda$ gives

$$\delta(\Delta\Pi) = 0 \tag{2}$$

where

$$\Delta\Pi = \frac{1}{2}\iiint_V \Delta\sigma_{\lambda\mu}\Delta\varepsilon_{\lambda\mu}dV + \frac{1}{2}\iiint_V \sigma_{\lambda\mu}(\Delta u_{k,\lambda}\Delta u_{k,\mu})dV - \iiint_V \Delta\bar{X}_\lambda \Delta u_\lambda dV$$

$$- \iint_{S_1} \Delta\bar{P}_\lambda \Delta u_\lambda dS + \left(\iiint_V \sigma_{\lambda\mu}\Delta\varepsilon_{\lambda\mu}dV - \iiint_V \bar{X}\Delta u_\lambda dV - \iint_{S_1} \bar{P}_\lambda \Delta u_\lambda dS\right) \tag{3}$$

In the Finite Element Method, $\Delta\Pi$ for a global system is defined as summation of $\Delta\Pi_E$ for each element, where $\Delta\Pi_E$ is calculated by using variables with respect to the local coordinates of the element.

From (3),

$$\Delta\Pi_E = \frac{1}{2}\Delta\delta^T\left(\iiint_{V_E} B^T D B dV\right)\Delta\delta + \frac{1}{2}\Delta\delta^T\left(\iiint_{V_E} \sigma_{\lambda\mu} G_{,\lambda}^T G_{,\mu} dV\right)\Delta\delta$$

$$- \Delta Q^T \Delta\delta + \left(\iiint_{V_E} \sigma^T B dV\right)\Delta\delta - Q^T\Delta\delta \tag{4}$$

where

$$\Delta\sigma = D\Delta\varepsilon, \quad \Delta\varepsilon = B\Delta\delta, \quad \Delta u = G\Delta\delta, \quad \Delta Q = \iiint_{V_E} G^T\Delta\bar{X}dV + \iint_{S_E} G^T\Delta\bar{P}dS$$

$\Delta\delta$: incremental nodal displacement vector with respect to local coordinates.

Performing the coordinates transformation of variables from the local to the global and then summing $\Delta\Pi_E$, $\Delta\Pi$ for the global system is obtained as

$$\Delta\Pi = \frac{1}{2}\Delta\delta_s^T K \Delta\delta_s + \frac{1}{2}\Delta\delta_s^T K_G \Delta\delta_s - \Delta Q_s^T \Delta\delta_s + (R^T \Delta\delta_s - Q_s^T \Delta\delta_s) \qquad (5)$$

where

$$K = \sum T_E^T \left(\iiint_{V_E} B^T D B \, dV \right) T_E, \qquad K_G = \sum T_E^T \left(\iiint_{V_E} \sigma_{\lambda\mu} G_{,\lambda}^T G_{,\mu} \, dV \right) T_E$$

$$R = \sum T_E \left(\iiint_{V_E} B^T \sigma \, dV \right)$$

T_E : coordinate transformation matrix
$\Delta\delta_s$: incremental nodal displacement vector with respect to global coordinates

From the principle of stationary,

$$(K + K_G)\Delta\delta_s = \Delta Q_s - (R - Q_s) \qquad (6)$$

The second term of the right hand side of the above equation can be considered to be caused by the incompleteness of the equilibrium conditions between external and internal forces at the previous step of configuration.

The problem treated here is combination of axial compression and uniaxial bending of columns and so, a first and a third order polynomials with respect to an axial coordinate are used as an axial and a lateral displacement function, respectively.

The stress-strain relation was assumed referring to results of material tests, to be perfectly plastic for the columns of R-sections and to be strain-hardening ($E_t = 1/100\,E = \text{constant}$) for the columns of H-sections (see fig. 3). The theoretical calculations of the maximum loads of the compression test specimens were performed by assuming symmetry of configuration about the midpoint of column length. The examples of subdivision of elements are shown in the fig. 4.

2.3. Comparison of Experiments with Calculations

Several examples of the relation between compressive load and central deflection are shown in figures 5 to 7, where the deflection is the additional one to the original configuration and the magnitude is measured by using a scale below the abscissa.

In the case of the column with small slenderness ratio as well as small initial deflection, the relation between compressive load and additional deflection is almost linear and the inclination is steep before initial yield load is attained. This tendency may be caused by the fact that the axial force component of the sectional forces is comparatively large. The compressive load decreases suddenly after the maximum load is attained (see R 4005 in figure 5).

While, in the case of the column with large slenderness ratio as well as large initial deflection, the relation between compressive load and additional deflection deviates already in the early stage considerably from linearity and reduction of the compressive load after the maximum load attained is hardly recognized (see R 12020 in figure 6).

The experimental and calculated maximum loads for all specimens are listed in table 1. The variation of the maximum loads due to the magnitudes of initial deflections is shown in figures 8 and 9 to take slenderness rations as a parameter. As to the calculations in these figures, for the tested specimens, the measured initial deflections were, of course, used as in-put data but otherwise the regular initial deflections were assumed.

Therefore, even if the slenderness ratios are kept constant, the calculated results are, strictly speaking, not necessary to be able to be connected by one contineous fair curve but in these figures, this attempt was done because the shapes of the initial deflections of all the specimens resembled closely the half wave mode of sine curve. According to these figures, almost all the calculated points are connected by each curve without excessive unnaturalness. In fig. 8, the Euler critical stress for the elastic range and the yield stress for the plastic range were taken respectively as an intersection of each curve with the ordinate and in figure 9, the same as above for the elastic range but natural extension of a curve for the plastic range were taken, respectively.

3. COLUMN CURVES OF COLUMNS WITH REGULAR INITIAL DEFLECTIONS

By using the curves in figures 8 and 9, column curves in figure 10 and figure 11 can be made where a/r is taken as a parameter. Figure 12 shows comparison of present calculations with Jezek's ones and in this case, a/l is taken as a parameter. Although Jezek's curves were obtained by assuming parabolic shapes of initial deflection symmetrical about the midpoint, both curves coincide well because Jezek's parabola is similar to the half wave mode of sine curve.

4. THE MAXIMUM COMPRESSIVE LOADS OF COLUMNS WITH IRREGULAR INITIAL DEFLECTIONS

It may be presumed that columns with regular initial deflections and with no rotational restrained at both ends are the weakest. However, it is necessary to know quantitative effects of shapes of initial deflections or of end restraints on the maximum loads of compressed columns. In this section, these kinds of problems are treated. The calculated results for columns with four kinds of irregular initial deflections and with fully rotational restraints at both ends are shown in table 2. In this table, the ratios of the maximum load of each column to the one of the column 8021, which is the column with regular initial deflection, are shown too.

According to this table, the compressive strength of the column 8022 and 8023 increasesby only few percents, but as to the column 8024, the increase is considerably large. However, it may be true that in an actual compression test of a column like 8024, mode change will occur at some intermediate stage of loading and the compressive load will not reach up to the value given in table 2.

In figure 13, the aspect of gradual variation of configuration of the column R 8025 is shown, where the shaded area indicates spread of the plastic zone and in figure 14, the same situation for the column R 8026 is shown.

5. THE MAXIMUM LOADS OF ECCENTRICALLY COMPRESSED COLUMNS WITH INITIAL DEFLECTIONS

In table 3, the effects of eccentricity of applied compressive forces on the maximum loads of straight columns and of columns with initial deflections are shown. The sectional shapes of columns are rectangular and their dimensions and material constants are the same as in table 2. Initial deflections are assumed to be the same regular shapes as before. From these results, it can be seen that even if the magnitude of eccentricity is the same as the one of initial deflection, the effect is different and also that when both eccentricity and initial deflection exist, the effect of these two kinds of imperfections cannot be obtained as the summation of the individual effect.

6. CONCLUSIONS

(1) The columns of R-section and H-section with initial deflections whose shapes are similar to the half wave mode of sine curve were compressed and the measured maximum loads were compared with the theoretical calculations by using the FEM. The experiments coincided well with the calculations with respect to both the load-deflection curves and the values of the maximum compressive loads.

(2) Column curves of R-section and H-section were made by using the calculated maximum loads.

(3) The maximum compressive loads of columns with several kinds of shapes of initial deflections were calculated and also the case of fixed end conditions was treated.

(4) The maximum loads of eccentrically compressed straight columns and of eccentrically compressed columns with initial deflections were calculated.

REFERENCES

(1) Jezek, K.
Die Festigkeit von Druckstaben aus Stahl, Julius Springer, 1937.

(2) Washizu, K.
Variational Methods in Elasticity and Plasticity, Pergamon Press, 1966.

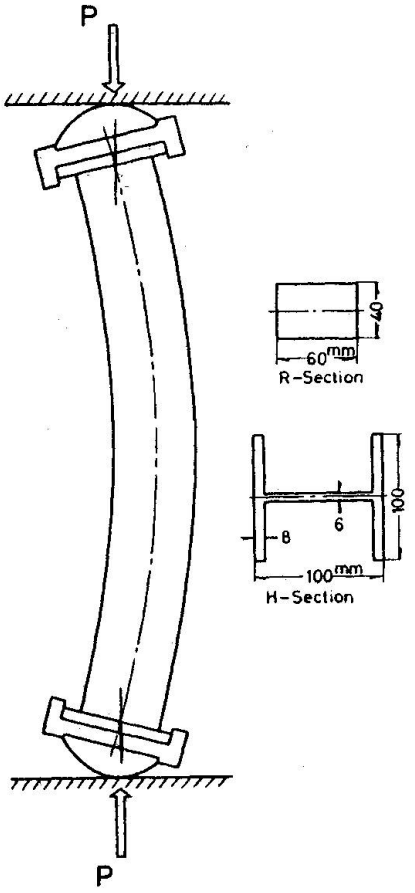

Fig.1 Compression Test Arrangement

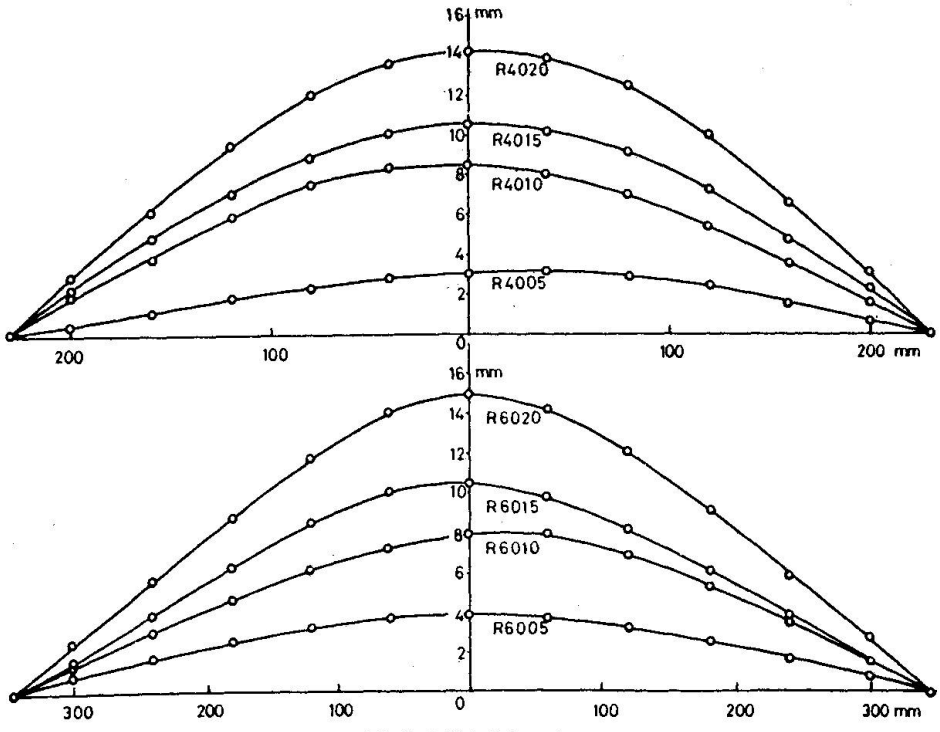

Fig.2 Initial Deformation

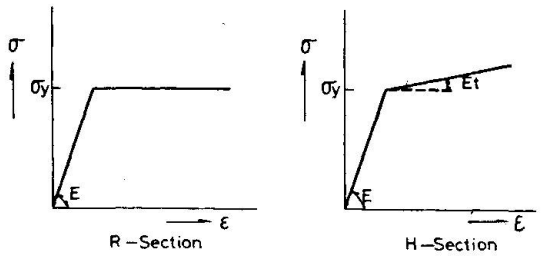

Fig 3 Assumed Stress Strain Diagrams

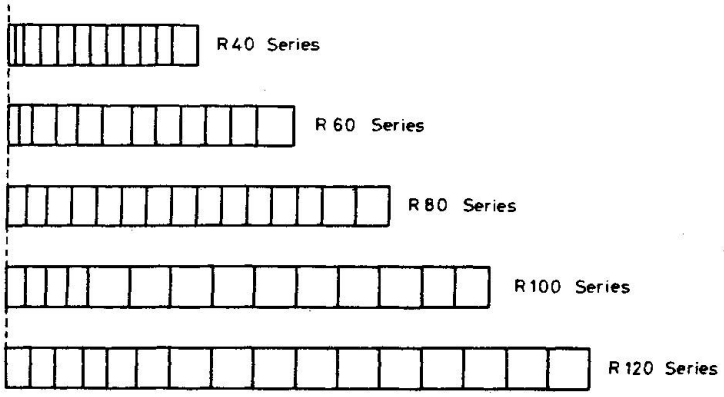

Fig 4 Element Subdivisions of R-Sections

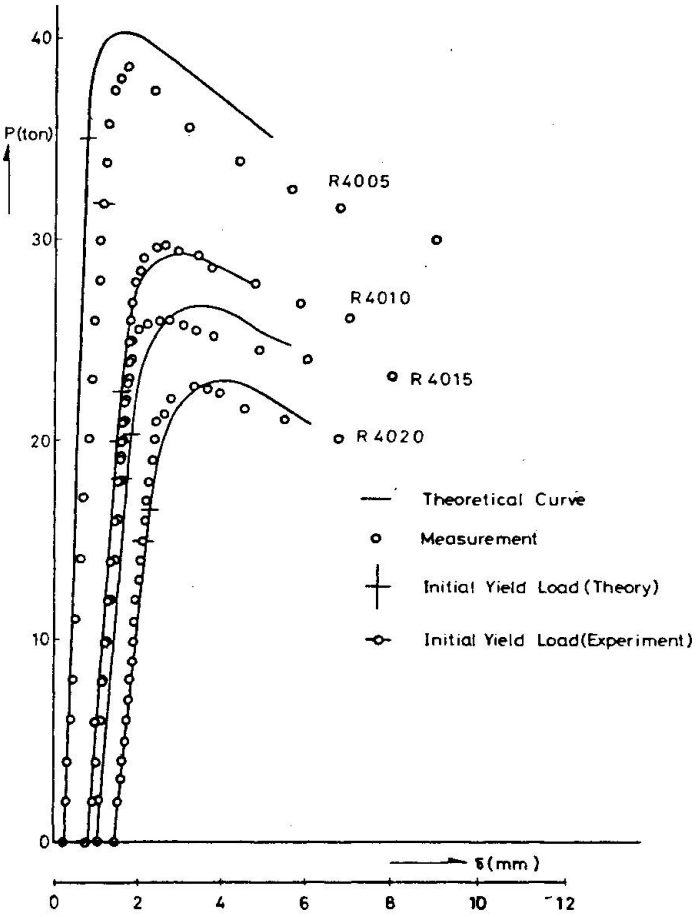

Fig 5 Load-Central Deflection Curves (R40 Series)

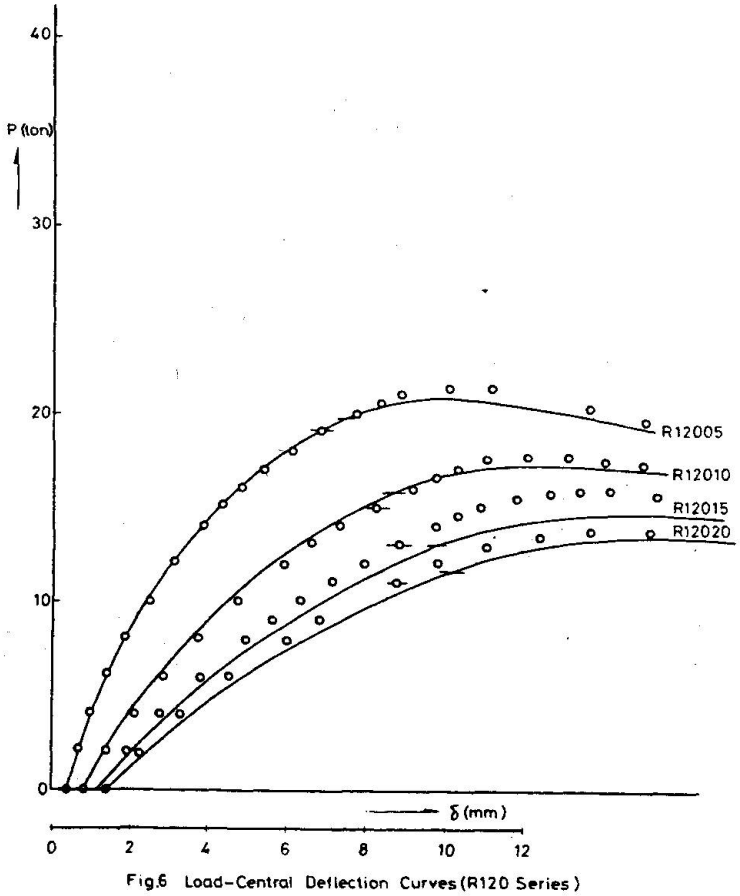

Fig.6 Load-Central Deflection Curves (R120 Series)

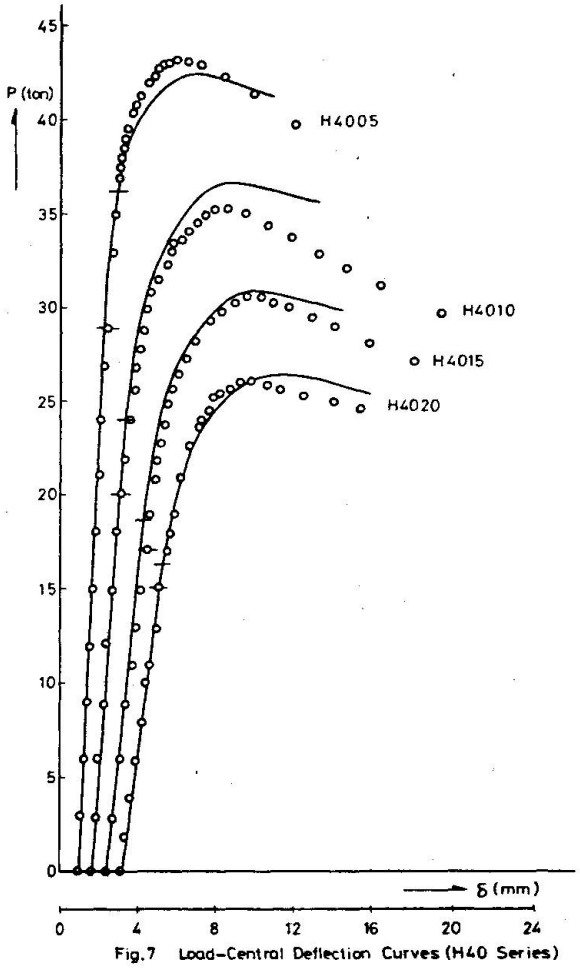

Fig.7 Load-Central Deflection Curves (H40 Series)

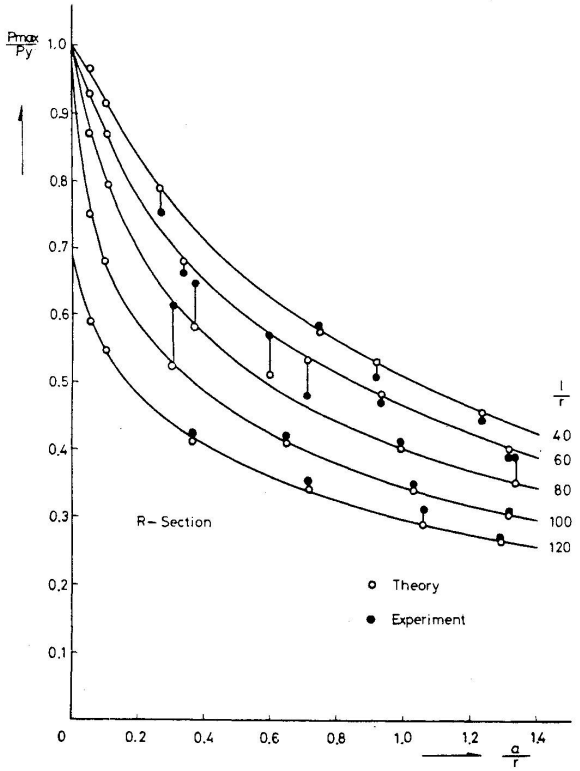

Fig.8 Relation between Maximum Loads and Initial Deflections of Rectangular Sections

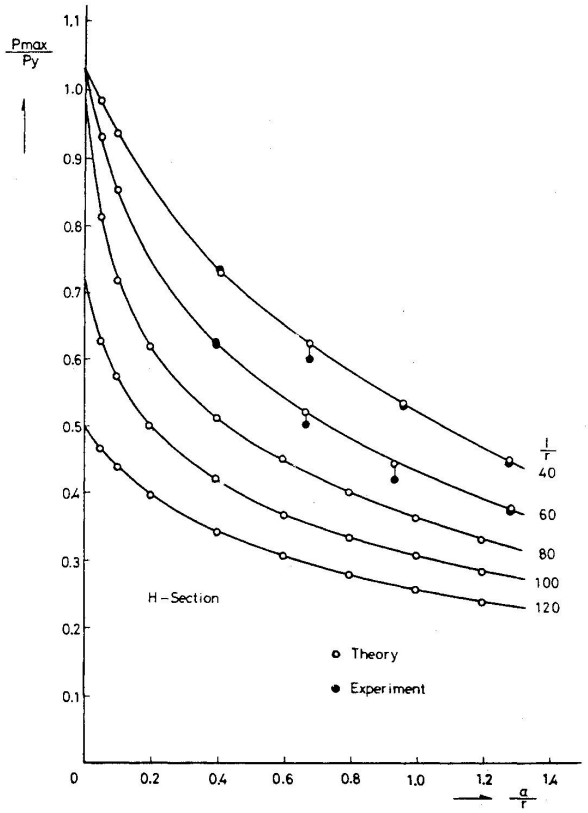

Fig.9 Relation between Maximum Loads and Initial Deflections of H-Sections

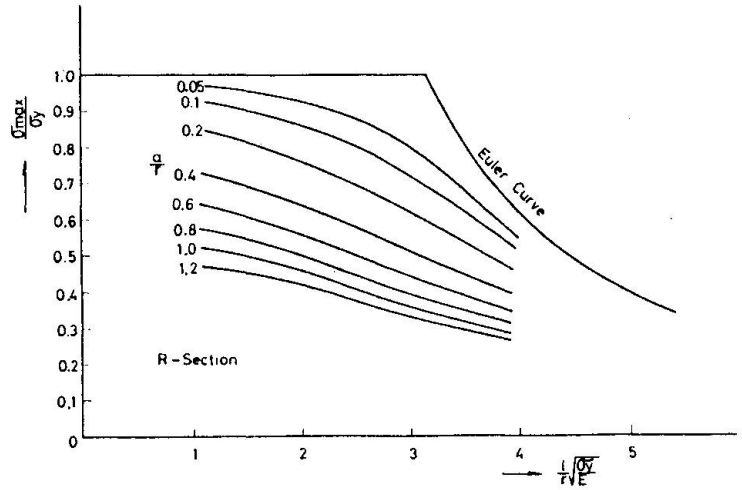

Fig.10 Column Curves of Rectangular Sections

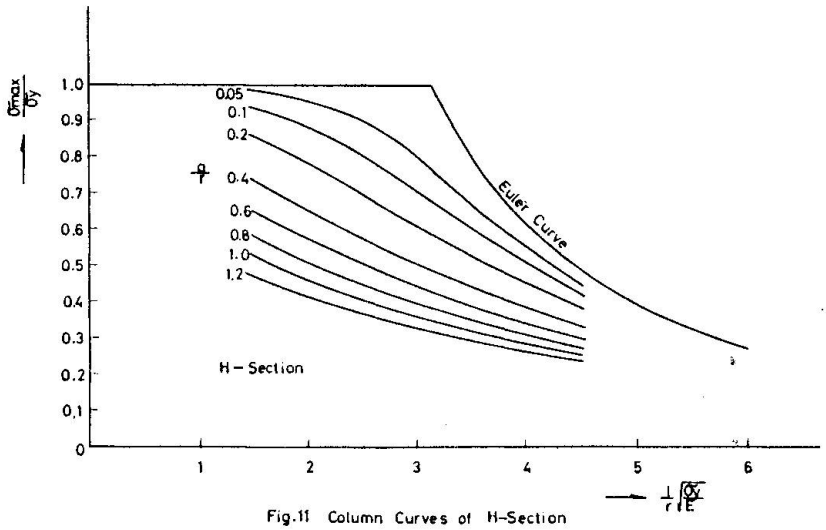

Fig.11 Column Curves of H-Section

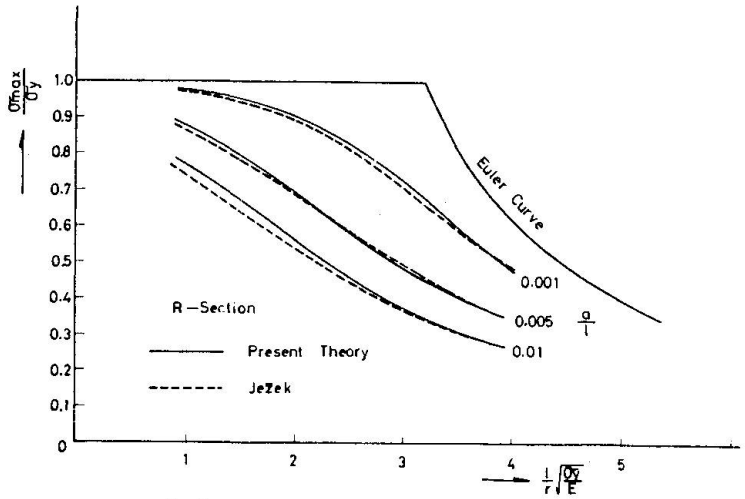

Fig.12 Comparison of Present Theory with Jeřek

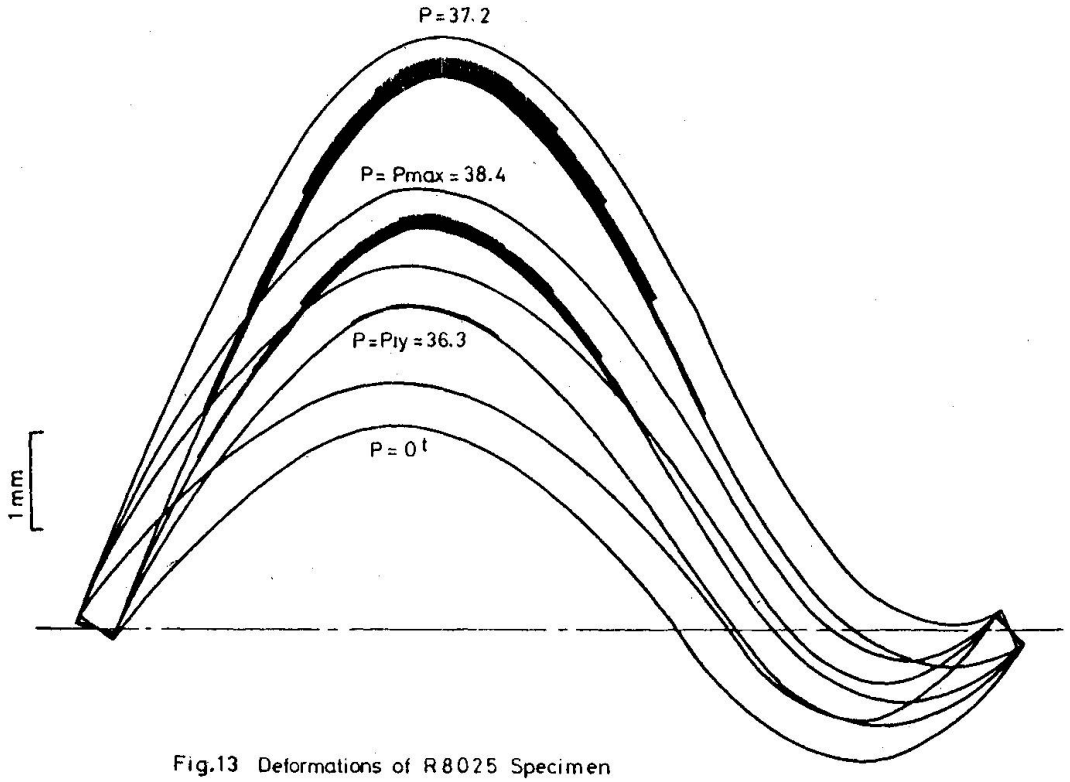

Fig.13 Deformations of R8025 Specimen

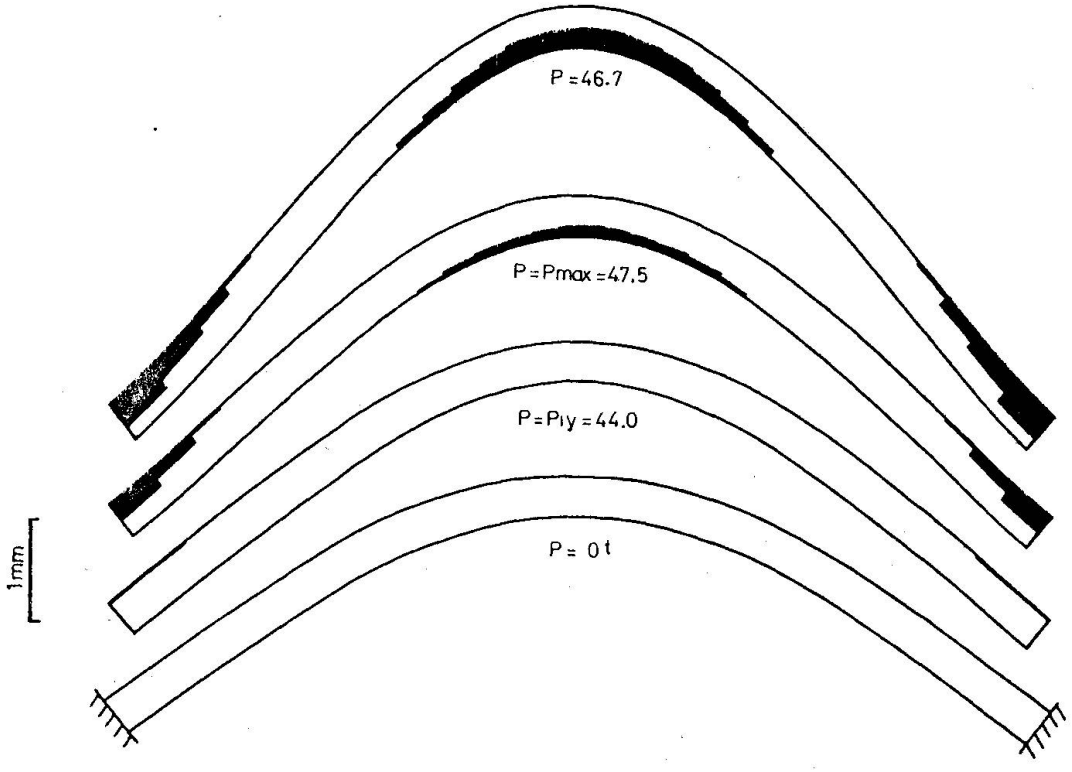

Fig. 14 Deformations of R8026 Specimen

Table 1 Experimental & Calculated Results

Specimen	Slenderness Ratio l/r	Initial Deflection Ratio a/r	Initial Deflection Ratio a/l	Experimental Maximum Load $(P_{max})_e$	Experimental Maximum Load $(P_{max})_e/P_y$	Theoretical Maximum Load $(P_{max})_t$	Theoretical Maximum Load $(P_{max})_t/P_y$	Error % $\frac{(P_{max})_t-(P_{max})_e}{(P_{max})_e}\times 100$
R4005	40	0.262	0.00655	38.6	0.757	40.3	0.791	4.3
R4010		0.742	0.0186	29.8	0.585	29.4	0.577	−1.2
R4015		0.912	0.0228	25.9	0.510	27.0	0.531	4.2
R4020		1.232	0.0308	22.6	0.444	23.2	0.456	2.5
R6005	60	0.341	0.00568	33.7	0.664	34.6	0.682	3.0
R6010		0.707	0.0118	24.5	0.482	27.2	0.535	11.2
R6015		0.931	0.0155	23.8	0.470	24.5	0.484	2.2
R6020		1.311	0.0218	19.8	0.391	20.4	0.403	2.9
R8005	80	0.368	0.00460	32.9	0.648	29.6	0.583	−10.2
R8010		0.592	0.00740	28.9	0.570	25.9	0.511	−10.4
R8015		0.993	0.0122	20.9	0.412	20.4	0.402	− 2.5
R8020		1.332	0.0167	19.8	0.391	17.7	0.350	−10.7
R10005	100	0.299	0.00299	31.2	0.617	26.5	0.524	−15.2
R10010		0.646	0.00646	21.3	0.421	20.7	0.409	− 2.9
R10015		1.027	0.0103	17.6	0.348	17.2	0.340	− 2.3
R10020		1.318	0.0132	15.7	0.310	15.3	0.303	− 2.6
R12005	120	0.365	0.00304	21.5	0.425	20.8	0.411	−3.1
R12010		0.711	0.00593	17.8	0.352	17.2	0.341	−2.6
R12015		1.058	0.00882	15.9	0.312	14.7	0.289	−7.5
R12020		1.283	0.0107	13.8	0.273	13.4	0.266	−2.6
H4005	40	0.410	0.0103	43.1	0.739	42.6	0.731	−1.1
H4010		0.679	0.0170	35.4	0.599	36.9	0.624	4.2
H4015		0.962	0.0241	30.7	0.525	31.1	0.531	1.2
H4020		1.283	0.0321	26.1	0.440	26.5	0.446	1.5
H6005	60	0.400	0.00667	36.3	0.620	36.5	0.624	0.7
H6010		0.669	0.0112	30.5	0.502	31.6	0.520	3.5
H6015		0.939	0.0157	25.1	0.418	26.6	0.443	5.9
H6020		1.291	0.0215	21.8	0.373	22.1	0.378	1.3

$\sigma_y = 21.5\ kg/mm^2$ for R–Section
$= 28.6\ kg/mm^2$ for H–Section

$E = 2.1\times10^4\ kg/mm^2$ for both Section

$E_t = 0\ kg/mm^2$ for R–Section
$= 2.1\times10^2\ kg/mm^2$ for H–Section

l : length
r : radius of gyration
a : initial deflection at midpoint

P_{max} : maximum load

P_y : compressiv yield load

Table 2. Calculated Results for Various Initial Deformations

Specimen	Initial Deformation	Slenderness Ratio l/r	Initial Deflection Ratio φ/r	Maximum Load		Maximum Load Ratio
				Pmax	Pmax/Py	
R 8021	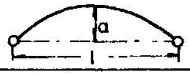	80	0.2	35.7 t	0.692	1.00
H 8021				37.2	0.618	1.00
R 8022				36.9	0.702	1.03
H 8022				38.8	0.645	1.04
R 8023	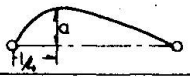			36.4	0.705	1.02
H 8023				38.3	0.637	1.03
R 8024	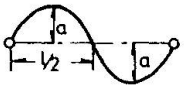			43.2	0.836	1.21
H 8024				48.7	0.809	1.31
R 8025				38.4	0.743	1.08
H 8025				40.5	0.674	1.08
R 8026	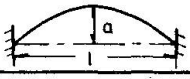			47.5	0.921	1.33
H 8026				55.4	0.921	1.49

σ_y = 21.5 kg/mm² E = 2.1x10⁴ kg/mm² Et = 0 kg/mm² for R-Section
= 28.6 kg/mm² = 2.1x10⁴ kg/mm² = 2.1x10² kg/mm² for H-Section

Table 3. Calculated Maximum Loads of Eccentrically Compressed Columns with Initial Deformations

Imperfection	Specimen	Calculated Condition	Slenderness Ratio l/r	Eccentricity or Initial Deflection	Maximum Load	
					Pmax	Pmax/Py
Eccentricity	R 8027	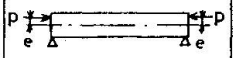	80	e = 0.2 mm	48.8 t	0.948
	R 8028			e = 1.0	41.1	0.795
	R 8029			e = 4.0	29.9	0.580
	R 8030	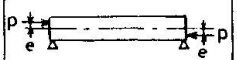		e = 0.2	51.6	1.000
	R 8031			e = 1.0	49.6	0.958
	R 8032			e = 4.0	41.8	0.811
Both Eccentricity and Initial Deflection	R 8033			e = 1.0 a = 1.0	36.5	0.708
	R 8034	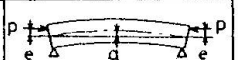		e = 1.0 a = 1.0	48.8	0.948
	R 8035	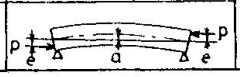		e = 1.0 a = 1.0	41.6	0.807

σ_y = 21.5 kg/mm² E = 2.1x10⁴ kg/mm² Et = 0 kg/mm²